Competing ground states in triple-layered $Sr_4Ru_3O_{10}$: Verging on itinerant ferromagnetism with critical fluctuations

G. Cao,[1] L. Balicas,[2] W. H. Song,[1,*] Y. P. Sun,[1,*] Y. Xin,[2] V. A. Bondarenko,[1] J. W. Brill,[1] S. Parkin,[3] and X. N. Lin[1]
[1]*Department of Physics and Astronomy, University of Kentucky, Lexington, Kentucky 40506, USA*
[2]*National High Magnetic Field Laboratory, Tallahassee, Florida 32310, USA*
[3]*Department of Chemistry, University of Kentucky, Lexington, Kentucky 40506, USA*
(Received 19 August 2003; revised manuscript received 4 September 2003; published 7 November 2003)

The triple-layered $Sr_4Ru_3O_{10}$ is characterized by an unexpectedly strong quasi-two dimensional characteristic, and a sharp metamagnetic transition and ferromagnetic behavior occurring within the basal plane and along the *c* axis, respectively. The interplane resistivity at magnetic field *B*, up to 32 T, exhibits very low-frequency quantum oscillations associated with the spin polarized state when *B* is parallel to the *c* axis, and a large magnetoresistivity accompanied by critical fluctuations governed by the metamagnetic transition when *B* is perpendicular to the *c* axis. The complex behavior evidenced in magnetization, specific heat, and resistivity presented is not characteristic of any obvious ground states, and points to a unusual state that shows a delicate balance between fluctuations and order. Implications of these results are discussed.

DOI: 10.1103/PhysRevB.68.174409 PACS number(s): 72.15.Gd, 71.27.+a, 75.47.−m

One of the major characteristics in the layered ruthenates, known as the Ruddlesden-Popper (RP) series, is that electronic and magnetic properties are critically linked to the lattice through the orbital degree of freedom. These layered ruthenates with strong magnetoelastic interactions are found to have an astonishing and distinctive dimensionality dependence of all physical properties that change systematically and profoundly with the number of RuO_6 octahedral layers.[1–17] Certainly, the RP series of the ruthenates represents a dramatic example of nature's success in engineering layered systems that are characterized by the coexistence of different kinds of order and the ground state instability. The RP series of the ruthenates has the general formula $(Ca,Sr)_{n+1}Ru_nO_{3n+1}$, where n (=1, 2, 3, and ∞) is the number of layers of corner sharing RuO_6 octahedra per formula unit. The progression of n from 1 to ∞ represents an increase in structural dimensionality as the number of nearest-neighbors increases from four for $n=1$ to six for $n=\infty$. It is found that the layered $Ca_{n+1}Ru_nO_{3n+1}$ ($n=1$, 2, and ∞) are all on the verge of metal-nonmetal transition and tend to be antiferromagnetic,[3–6,11–15] whereas the isostructural and isoelectronic $Sr_{n+1}Ru_nO_{3n+1}$ ($n=1$, 2, 3, and ∞) are metallic and seemingly inclined to be ferromagnetic with a notable exception being Sr_2RuO_4, that displays unconventional superconductivity.[1,8–11,15–17] The sensitivity of Fermi surface topography to the lattice or structural distortions is unusually strong in that no such behavior has been observed in other transition metal RP systems where the ground state can be readily and drastically changed by the isostructural and isoelectronic cation substitution (Ca or Sr). It is this ground state instability that drives the interesting behavior and characterizes the layered ruthenates.[1–17]

$Sr_{n+1}Ru_nO_{3n+1}$, besides the *p*-wave superconductor Sr_2RuO_4 ($n=1$),[1] also includes the strongly enhanced paramagnet $Sr_3Ru_2O_7$ ($n=2$, $T_M=18$ K),[8] and the itinerant ferromagnet $SrRuO_3$ ($n=\infty$, $T_C=165$ K).[11] The bilayered $Sr_3Ru_2O_7$ demonstrates behavior consistent with proximity to a metamagnetic quantum critical point,[9,10] and the infinite-layered $SrRuO_3$ is an itinerant ferromagnet with a reduced magnetic moment of $1.1\mu_B$/Ru.[11] With $n=3$ intermediate between $n=2$ and ∞, the triple-layered $Sr_4Ru_3O_{10}$ shows ferromagnetic behavior with $T_C=105$ K,[17] followed by an additional magnetic transition at $T_M=50$ K primarily along the *c* axis. While the evolution of (ferro)magnetism in $Sr_{n+1}Ru_nO_{3n+1}$ apparently reflects variations in the Fermi surface topography consistent with the progression of n from 1 to ∞, transport and thermodynamic properties observed in this study suggest that $Sr_4Ru_3O_{10}$ is poised between an itinerant metamagnetic state and an itinerant ferromagnetic state that characterize its closest neighbors $Sr_3Ru_2O_7$ and $SrRuO_3$, respectively. The anisotropic and complex magnetism is accompanied by critical fluctuations and an equally anisotropic and complex transport behavior including a large tunneling magnetoresistance and low frequency quantum oscillations that are uncommon in oxides and not discerned in $Sr_3Ru_2O_7$. In this paper, we report on the resistivity, magnetization, and specific heat of single crystal $Sr_4Ru_3O_{10}$ as a function of temperature and magnetic field.

The single crystals studied were grown using flux techniques and characterized by single crystal x-ray diffraction at various temperatures, EDX, and TEM, which suggest no intergrowth. From the Dingle plot the Dingle temperature $T_D=h/4\pi^2k_B\tau$, a measure of the scattering time, is estimated to be $T_D=3.2\pm0.8$ K comparable to those of good organic metals, whose T_D varies from 0.5 to 3.5 K, indicating a high quality of single crystals. High field (>9 T) measurements were performed at the National High Magnetic Field Laboratory through a user program.

The orthorhombic unit cell of $Sr_4Ru_3O_{10}$ is composed of triple layers of corner-shared RuO_6 octahedra separated by double rock-salt layers of Sr-O.[17] The triple-layered feature is clearly illustrated in the TEM image and the diffraction pattern taken along [110] direction shown in Fig. 1. Remarkably, RuO_6 octahedra in the outer layers are elongated at low temperatures,[17] which affects d_{zx} and d_{yz} orbitals, and the RuO_6 octohedra in the outer layers of each triple layer are

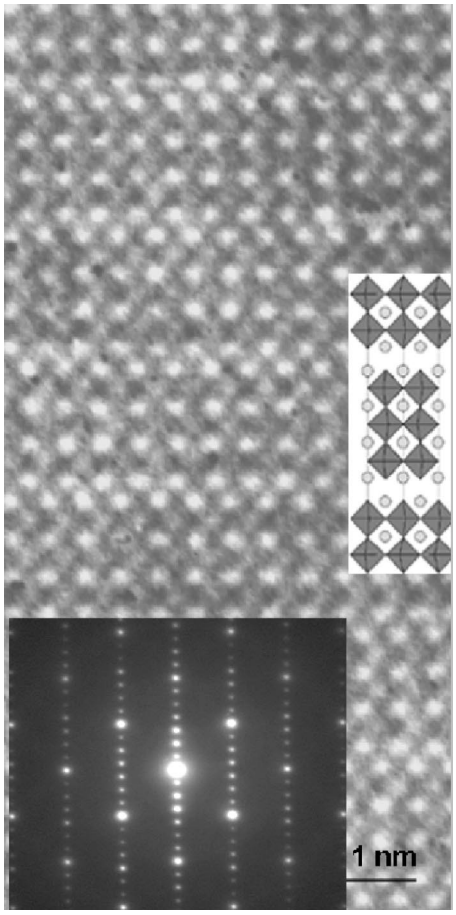

FIG. 1. High resolution TEM image and diffraction pattern taken along the [110] direction (lower left), where the triple-layered feature is clearly illustrated.

rotated by an average of 5.6° around the *c* axis, whereas the octahedra of the central layers are rotated by an average of 11.0° in the opposite direction,[17] which may drive ferromagnetic coupling.

Displayed in Fig. 2 are the temperature dependences of the magnetization M and resistivity ρ, for the basal plane and the c axis, and the specific heat C measured with accalorimetry[18,19] and normalized by a low-temperature value measured earlier.[20] In Fig. 2(a), M for the c axis at $B=0.01$ T shows a Curie temperature T_C at 105 K, which is then followed by a sharp transition at $T_M=50$ K (magnetic fields B and H are scaled versions of each other, the former measured in Tesla and the latter measured in A/m. B is used here). The irreversibility of M becomes large below T_M, consistent with a ferromagnetic behavior. However, M for the basal plane exhibits only a weak cusp at T_C, but a pronounced peak at T_M, resembling an antiferromagneticlike behavior (see the inset), and showing a much smaller irreversibility. While the strong competition between ferromagnetic and antiferromagnetic coupling is always a major characteristic of the ruthenates, this behavior is not entirely expected in that the evolution of magnetism in $Sr_{n+1}Ru_nO_{3n+1}$ for $n=1$, 2, and ∞, would suggest an increasingly strong, but less anisotropic, coupling favorable for ferromagnetism as n increases and as the orthorhombicity and the RuO_6 rotation are present.[21,22]

The magnetic susceptibility for 150–350 K obeys the Curie-Weiss law, yielding highly anisotropic Pauli susceptibilities χ_o of 4.1×10^{-3} and 1.4×10^{-4} emu/mole for the c axis and the basal plane, respectively. (The Curie-Weiss law holds for paramagnetic metals that are in the vicinity of the ferromagnetic instability[23]). The largely enhanced χ_o for the

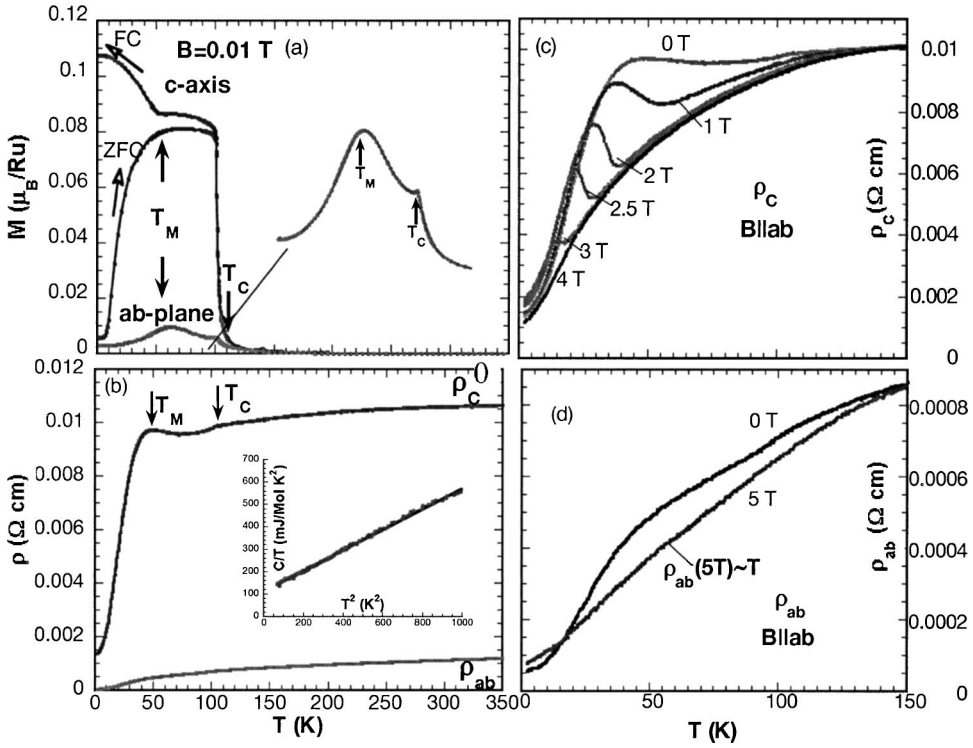

FIG. 2. (a) Magnetization as a function of temperature for the basal plane and the c axis at $B=0.01$ T. Inset: Enlarged M (T) for the basal plane below 150 K without axes to clarify the antiferromagneticlike behavior. (b) Basal plane resistivity ρ_{ab} and interplane resistivity ρ_c as functions of temperature. Inset: specific heat normalized by T, C/T, vs T^2 for $T\leqslant31$ K. (c) ρ_c vs T at a few representative magnetic fields B parallel to the basal plane. (d) ρ_{ab} vs T at $B=0$ and 5 T parallel to the basal plane.

TABLE I. Summary of some parameters for the *c* axis and the basal plane.

Parameter	*c* axis	Basal plane
χ_o (memu/mole)	4.1	0.13
μ_{eff} (μ_B/Ru)	2.62	2.37
Curie-Weiss temperature (K)	122	118
μ_s (μ_B/Ru) (at. 1.7 K)	1.13	0.9
μ_{eff}/μ_s	2.32	2.63
B_c (T) (at 1.7 K)	0.2	3.5
ρ_o ($\mu\Omega$ cm)	1308 (0 T)	54 (0 T)
A ($\mu\Omega$ cm/K^2)	10.4 (0 T)	0.34 (0 T)
R_w	2.4	0.08
A/γ^2 ($\mu\Omega$ cm/(mJ/K^2 mol)^2)	85.9×10^{-5}	2.8×10^{-5}

c axis suggests a large density of states near the Fermi surface, in accord with the Stoner criterion for ferromagnetism that occurs along the *c* axis. On the other hand, χ_o for the basal plane is more than an order of magnitude smaller than that of the *c* axis, implying a less energetically favorable condition for ferromagnetism so evident in Fig. 2(a). The surprisingly large anisotropic χ_o ($\chi_o^c/\chi_o^{ab}=29$) certainly points to the highly anisotropic density of states near the Fermi surface. Measurements of specific heat $C(T)$ yields the electric specific heat $\gamma=109$ mJ/mol K^2. The Wilson ratio $R_w(=3\pi^2k\chi_o/\mu_B^2\gamma)$ is found to be 2.4 and 0.08 for the *c* axis and the basal plane, respectively, assuming γ probes the average value of the renormalization effect over the entire Fermi surface. All these results reflect the high density of states for the *c* axis that brings about the ferromagnetic behavior, and yet the much smaller density of states for the basal plane that is not large enough to cause ferromagnetic instability (see Table I for comparisons). It is thus not entirely surprising that $C(T)$ exhibits a perfect T^3 dependence below 30 K without any visible deviation, e.g., $T^{3/2}$-dependence expected for (three-dimensional) ferromagnetic spin waves [see the inset of Fig. 2(b)], although the low-temperature specific heat is currently being reexamined more closely.[19]

Shown in Fig. 2(b) is the resistivity ρ vs temperature for the *c* axis and the basal plane. ρ_c exhibits anomalies corresponding to T_C and T_M, whereas ρ_{ab} shows weaker ones at T_C and T_M (not obvious in the figures). The most prominent features are the unexpectedly large anisotropy and unusual temperature dependence of ρ_c. The ratio of ρ_c/ρ_{ab} ranges from nearly 30 at 2 K to 10 at 350 K, a still quite two-dimensional characteristic despite of the triple layered structure. ρ_c precipitously drops by nearly an order of magnitude from 50 to 2 K. Such a drop in ρ_c is somewhat similar to that of Sr_2RuO_4 and $Sr_3Ru_2O_7$ but more pronounced and less anticipated because the triple-layered structure should be more energetically favorable for interplane hopping. It is likely to be due to a drastic reduction of spin scattering as the system becomes more spin polarized below T_M, evidenced in Fig. 2(a). This is supported by the data shown in Fig. 2(c) where the anomaly at T_M rapidly decreases with increasing B applied parallel to the basal plane and eventually vanishes at

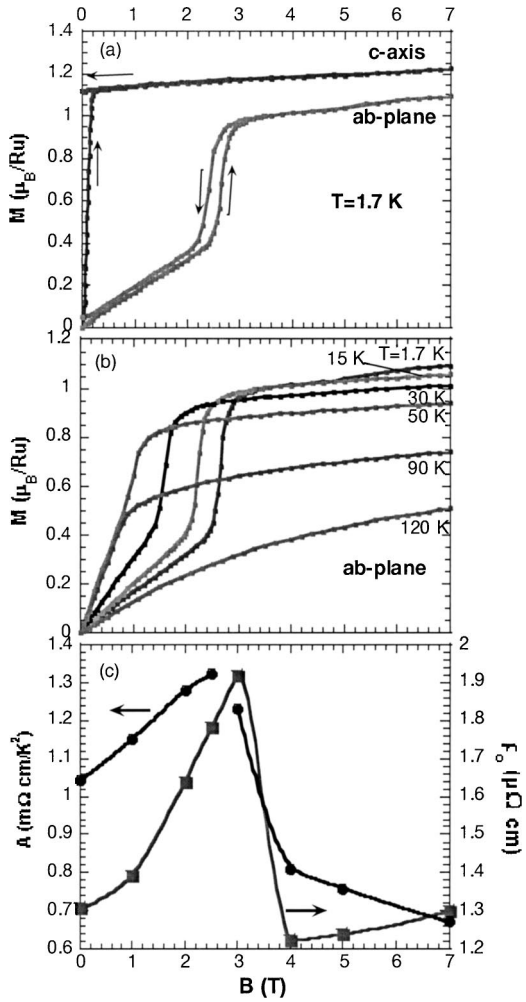

FIG. 3. (a) Isothermal magnetization as a function of B at $T=1.7$ K for the basal plane and the *c* axis. (b) Basal plane isothermal magnetization at $T=1.7$, 15, 30, 50, 90, and 120 K. Note that metamagnetic transition decreases with increasing T and vanishes at $T>50$ K. (c) Magnetic field dependence of the coefficient A and residual ρ_o obtained from the data shown in Fig. 2(c).

$B=4$ T. The brief nonmetallic behavior (negative slope) seen between $T_M(=50$ K) and 70 K may be associated with the elongated RuO_6 octahedra in the outer layers at low temperatures.[17] Our recent single crystal diffraction also shows that the *c* axis is elongated by approximately 0.2% from 300 to 90 K. Such a lengthened *c* axis lifts the degeneracy of the t_{2g} orbitals and narrows the d_{xz} and d_{yz} bands relative to the d_{xy} bond weakening the interplane hopping. This point is in line with the high density of states indicated by χ_o^c. It is also possible that the system undergoes a structural transition such as a rotation of RuO_6 below T_M. The domain wall pinning at $T<T_M$ may become stronger, giving rise to the stronger hysteresis as seen in Fig. 2. The reduced symmetry below T_M breaks some symmetry restriction and increases the interlayer tunneling, thus reducing the *c*-axis resistivity. The transition and the rotation are strongly affected by B because of the strong spin-orbit coupling, giving rise to the behavior seen in Fig. 2(c).

At low temperatures, Fermi liquid behavior survives as

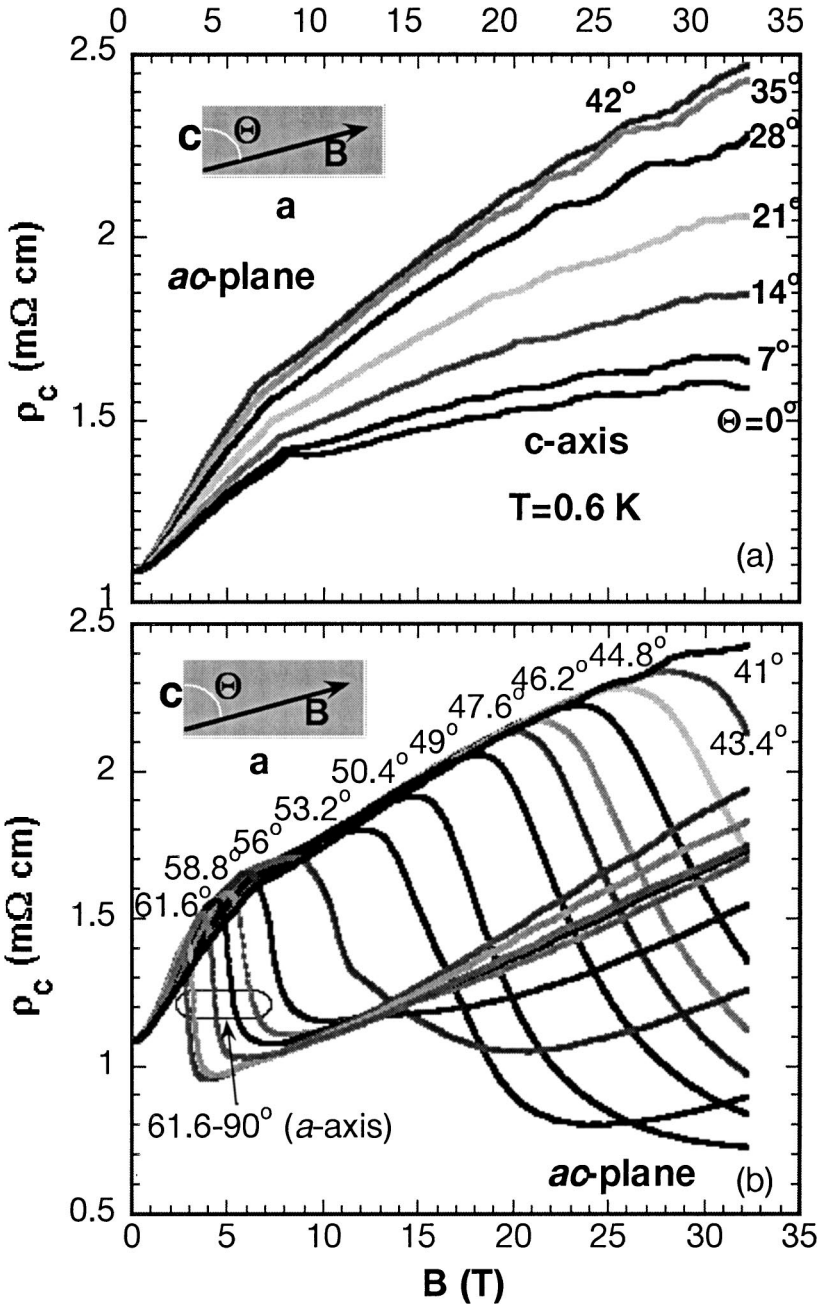

FIG. 4. ρ_c at $T=0.6$ K as a function of B rotating from the c axis to the basal plane.

both ρ_c and ρ_{ab} obey $\rho=\rho_o+AT^2$ for the significant regime 2–15 K, with $\rho_{oc}=1.30\times10^{-3}$ Ω cm, $\rho_{oab}=5.4\times10^{-5}$ Ω cm (indicative of the high purity of the sample[18]), $A_c=1.04\times10^{-5}$ Ω cm/K^2, and $A_{ab}=3.4\times10^{-7}$ Ω cm/K^2. The c-axis values are close to those of $Sr_3Ru_2O_7$,[8] but the basal plane values are about an order larger; i.e., while triple layer $Sr_4Ru_3O_{10}$ has a more isotropic resistivity than double layer $Sr_3Ru_2O_7$, it is not because of better transport along c but because of more basal plane scattering. It is also surprising that the anisotropies in A (~31) and ρ_o (~24) are similar, since the latter depends only on the band mass and elastic scattering rate, while A depends on the interacting quasiparticle effective mass and inelastic rate, and, unlike $Sr_3Ru_2O_7$, the susceptibility is anisotropic. In any case, all these parameters, tabulated in Table I, clearly suggest that the Fermi surface remains anisotropic in this triple layer material. The value of A_c is much larger than that of ordinary Fermi liquids and, along with the c-axis Wilson ratio $R_W=2.4$, suggests strong correlation effects in this direction.

Consistent with the above results, both ρ_c and ρ_{ab} show neither a $T^{3/2}$ nor $T^{5/3}$ dependence in the vicinity of the magnetic anomalies expected for a three-dimensional antiferromagnet and ferromagnet, respectively.[24,25] Beyond the transition regions, ρ_{ab} shows essentially linear temperature dependence for temperature ranges of 18–38, 50–100, and 140–350 K, suggesting strong fluctuations. Furthermore, ρ_{ab} shows negative magnetoresistivity, defined as $\Delta\rho/\rho(0T)$, that reaches as large as 28% in the vicinity of and below T_M at $B=5$ T applied parallel to the basal plane [see Fig. 2(d)]. This is important because spin scattering is expected to be

minimized at $B=0$ in itinerant ferromagnets where electrons find the path of least dissipation to cross the sample, and thus positive magnetoresistance is anticipated in the presence of B which forces electrons to take a different path. The observed negative magnetoresistance of ρ_{ab} is a clear indication of large spin fluctuations existing in a non-ferromagnetic state. This point is consistent with the T dependence of ρ_{ab} at 5 T for 10–100 K shown in Fig. 2(d).

Indeed, as shown in Figs. 3(a) and 3(b), where the isothermal magnetization M for the basal plane and the c axis for various temperatures is plotted,[26] spins along the c axis are readily polarized at only 0.2 T, yielding a saturation moment M_s of $1.13\mu_B$/Ru extrapolated to $B=0$ for $T=1.7$ K, slightly more than a half of $2\mu_B$/Ru expected for an $S=1$ system. This M_s is comparable with that for $SrRuO_3$ whose easy axis lies within the basal plane,[11] but the distinct field dependence of M shown in Fig. 3 is vastly different from that of $SrRuO_3$ (Ref. 11) and $Sr_3Ru_2O_7$.[8] While the irreversibility of M for the c axis is typical of a ferromagnet, M for the basal plane shows a sharp metamagnetic transition, B_c. Clearly, B_c decreases and broadens with increasing temperature, and vanishes at $T_M=50$ K [Fig. 2(b)]. The metamagnetism is observed in $Sr_3Ru_2O_7$ for both the basal plane and the c axis with broader and higher B_c, which drives the ground state from a paramagnetic state at low fields to an induced ferromagnetic state at high fields.[9,10] Itinerant metamagnets are often characterized by a maximum in the temperature dependence of the paramagnetic susceptibility.[25] In light of the itinerant and unusual magnetic character with ferromagnetism along the c axis and the antiferromagnetic-like behavior within the basal plane shown in Figs. 2 and 3, it is intriguing as to whether this metamagnetic transition represents a transition between a paramagnetic and ferromagnetic state similar to that of itinerant metamagnets such as $Sr_3Ru_2O_7$, or a transition that characterizes a change from an antiferromagnetic state at low fields to a ferromagnetic state at higher fields, a process that manifests strong competing interactions between ferromagnetic and antiferromagnetic couplings, and is known to often occur in insulators.[27] It is clear, however, that this exotic behavior in $Sr_4Ru_3O_{10}$ is not characteristic of either a robust ferromagnet or an antiferromagnet, implying the close energies of the states. It is worth pointing out that the anomalous magnetic behavior is often related to structural changes, and it is possible that the magnetic behavior observed is driven by structural changes at temperatures below 50 K, which are yet to be observed.

This line of reasoning is reinforced by the fact that the c-axis transport properties appear to be dominated by the metamagnetic transition. Exhibited in Fig. 3(c) are the magnetic field dependences of A_c and ρ_{oc}, obtained by fitting the data below 15 K [see Fig. 2(c)] to $\rho_c=\rho_{oc}+A_cT^{\alpha}$, for $0 \leqslant B \leqslant 7$ T. $\alpha=2$, except between 2.7 and 2.9 T, for which the anomalous exponent $\alpha=1.2$, as also found in $Ca_3Ru_2O_7$ (Ref. 4) and in heavy Fermion compounds near quantum critical points.[28,29] The sharp peaking of both A_c and ρ_{oc} suggests large changes in carrier density and is strikingly similar to that in $Sr_3Ru_2O_7$ near 7.85 T below 0.35 K, the key evidence for its magnetic field-tuned quantum criticality.[10]

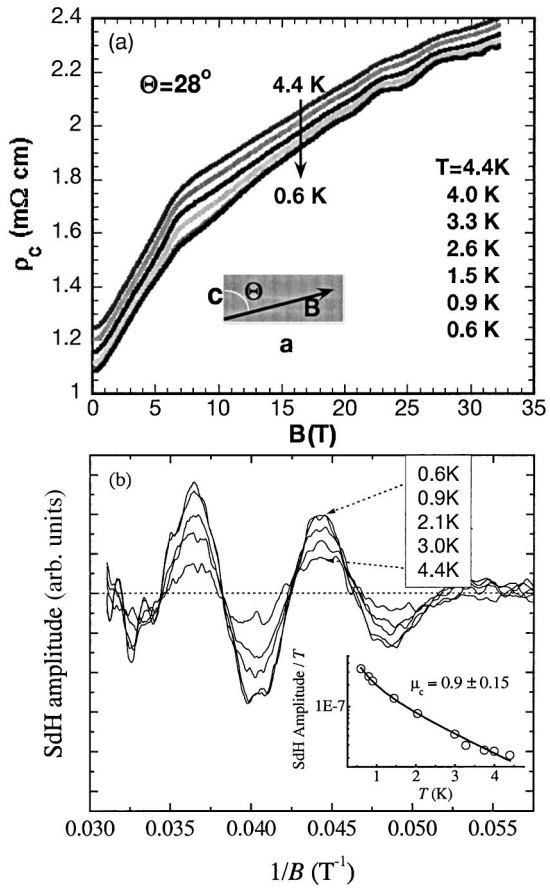

FIG. 5. (a) ρ_c as a function of B at $\Theta=28°$ for a few representative temperatures. (b) Shubnikov–de Hass effect as a function of B^{-1} for various temperatures specified. Inset: Temperature dependence of the SdH magnitude normalized by T yields the cyclotron effective mass μ_c.

The transport properties driven by the metamagnetism is also illustrated in Fig. 4, where ρ_c is plotted as a function of B rotating from the c axis to the a axis (no difference is discerned for B parallel to the a- and b-axes). Θ is defined as an angle between the c axis and B. Noticeably, ρ_c rises initially with increasing Θ by nearly 40% from 1.58 mΩ cm at $\Theta=0°$ ($B\|c$ or the easy axis) to 2.47 mΩ cm at $\Theta=42°$ at 32 T. This behavior suggests minimized scattering at $\Theta=0$ where spins are largely polarized along the c-axis. As Θ reaches $\Theta=43.4°$ ρ_c starts to show negative magnetoresistivity characterized by a sudden drop at a critical field B_c. This B_c systematically decreases with increasing Θ, apparently corresponding to the metamagnetic transition that leads to the rapid spin polarization evidenced in M when $B\|ab$. The abrupt metamagnetic transition yields a negative magnetoresistivity ratio of more than 60%. Such a large interplane magnetoresistivity is believed to be due to a tunneling effect facilitated by a field-induced coherent motion of spin-polarized electrons between Ru-O planes, which is also seen in bilayered systems such as $Ca_3Ru_2O_7$ (Refs. 3 and 4) and $La_{2-2x}Sr_{1+2x}Mn_2O_7$.[30] Evidently, the metamagnetic transition B_c reconstructs the Fermi surface and sharply divides the large negative magnetoresistivity and quantum oscillations as can clearly be seen in Figs. 4(a) and 4(b). The

Shubnikov–de Haas (SdH) effect occurs at low Θ and becomes the most pronounced at $\Theta = 28°$ shown in Fig. 4(a). The rapid disappearance of the SdH effect with changing Θ reflects the quite two-dimensional nature of the Fermi surface although the SdH frequency as a function of $\cos\Theta^{-1}$ is to be established through further investigations.

The SdH effect expectedly becomes stronger as temperature decreases as shown in Fig. 5(a) where ρ_c vs B with $\Theta = 28°$ is plotted. Shown in Fig. 5(b) is the amplitude of the SdH signal[31] as a function of B^{-1} for a few representative temperatures. The SdH signal is defined as $(\sigma - \sigma_b)/\sigma_b$, where σ is the conductivity whereas σ_b is the background conductivity. As can be seen the detected frequency is low, and only a few oscillations are observed in the entire field ranging up to 32 T. Consequently, the usual fast Fourier analysis is inapplicable to the present case. The frequencies can, however, be determined by directly measuring the period of the oscillations, for example, for $B^{-1} \leqslant 0.05\ \mathrm{T}^{-1}$. The data analyses[31] reveal a frequency $F = 123 \pm T$, which, based on the crystallographic data of $Sr_4Ru_3O_{10}$ (Ref. 17) and the Onsager relation $F_0 = A(h/4\pi^2 e)$ (e is the electron charge), corresponds to an area of only 0.9% of the first Brillouin zone. The inset shows the amplitude of the SdH signal measured at the highest fields as a function of temperature. The solid line is a fit to the Lifshitz-Kosevich formulas, $x/\sin hx$, where $x = 14.69\mu_c T/B$.[32] The nearly perfect fit yields a cyclotron effective mass $\mu_c = 0.9 \pm 0.15$. The cyclotronic effective mass smaller than expected is attributed to the fact that it has been difficult to resolve the heavier effective masses in quantum oscillation experiments.[4,33] This is also seen in $Ca_3Ru_2O_7$,[3,4] and is quite common in heavy fermion systems.[31]

What makes this triple layered ruthenate intriguing is that it shows a delicate balance between fluctuations and order. This study reveals sound evidence of critical fluctuations driven by the metamagnetic transition in one direction and by ferromagnetic behavior in the other direction. The anisotropic transport properties seem to be critically linked to the metamagnetic transition that leads to the Fermi surface reconstruction evidenced in the quantum oscillations and the large magnetoresistance. All results presented suggest a behavior that is characterized by an exotic ground state with proximity to the itinerant ferromagnetic instability and the possible quantum critical point. $Sr_4Ru_3O_{10}$ with readily tunable parameters opens an avenue to study the itinerant ferromagnetism and quantum criticality so imperative to highly correlated electrons.

We are grateful to Professor Ganpathy Murthy for very helpful discussions. This work was supported by NSF Grant No. DMR-0240813 (G.C.), NSF Grant No. DMR-0100572 (J.W.B.), and the NHMFL under Cooperative Agreement No. DMR-0084173 (Y.X.).

*Permanent address: Institute of Solid State Physics, Chinese Academy of Sciences, Hefei 230031, Anhui, People's Republic of China.

[1] Y. Maeno, T. M. Rice, and M. Sigrist, Phys. Today **54** (1), 42 (2001).
[2] D. Singh and I. I. Mazin, Phys. Rev. B **56**, 2556 (1997).
[3] G. Cao, L. Balicas, Y. Xin, E. Dagotto, J. E. Crow, C. S. Nelson, and D. F. Agterberg, Phys. Rev. B **67**, 060406(R) (2003).
[4] G. Cao, L. Balicas, Y. Xin, J. E. Crow, and C. S. Nelson, Phys. Rev. B **67**, 184405 (2003).
[5] G. Cao, S. McCall, J. E. Crow, and R. P. Guertin, Phys. Rev. Lett. **78**, 1751 (1997).
[6] G. Cao, K. Abbound, S. McCall, J. E. Crow, and R. P. Guertin, Phys. Rev. B **62**, 998 (2000).
[7] G. Cao, S. McCall, M. Shepard, J. E. Crow, and R. P. Guertin, Phys. Rev. B **56**, R2916 (1997).
[8] S. I. Ikeda, Y. Maeno, S. Nakatsuji, M. Kosaka, and Y. Uwatoko, Phys. Rev. B **62**, R6089 (2000).
[9] R. P. Perry, L. M. Galvin, S. A. Grigera, A. J. Schofield, A. P. Mackenzie, M. Chiao, S. R. Julian, S. I. Ikeda, S. Nakatsuji, and Y. Maeno, Phys. Rev. Lett. **86**, 2661 (2001).
[10] S. A. Grigera, R. P. Perry, A. J. Schofield, M. Chiao, S. R. Julian, G. G. Lonzarich, S. I. Ikeda, Y. Maeno, A. J. Millis, and A. P. Mackenzie, Science **294**, 329 (2001).
[11] G. Cao, S. McCall, M. Shepard, J. E. Crow, and R. P. Guertin, Phys. Rev. B **56**, 321 (1997).
[12] C. S. Alexander, G. Cao, V. Dobrosavljevic, E. Lochner, S. McCall, J. E. Crow, and P. R. Guertin, Phys. Rev. B **60**, R8422 (1999).
[13] G. Cao, S. McCall, M. Shepard, J. E. Crow, and R. P. Guertin, Phys. Rev. B **56**, R2916 (1997).
[14] G. Cao, S. McCall, V. Dobrosavljevic, C. S. Alexander, J. E. Crow, and R. P. Guertin, Phys. Rev. B **61**, R5053 (2000).
[15] G. Cao, S. McCall, J. Bolivar, M. Shepard, F. Freibert, and J. E. Crow, Phys. Rev. B **54**, 15 144 (1996).
[16] G. Cao, F. Freibert, and J. E. Crow, J. Appl. Phys. **81**, 3884 (1997).
[17] M. Crawford, R. L. Harlow, W. Marshall, Z. Li, G. Cao, R. L. Lindstrom, Q. Huang, and J. W. Lynn, Phys. Rev. B **65**, 214412 (2002).
[18] M. Chung, E. Figueroa, Y.-K. Kuo, Y. Wang, J. W. Brill, T. Burgin, and L. K. Montgomery, Phys. Rev. B **48**, 9256 (1993).
[19] V. A. Bondarenko, J. W. Brill, and G. Cao (unpublished).
[20] S. McCall (private communication).
[21] D. J. Singh and I. I. Mazin, Phys. Rev. B **63**, 165101 (2001).
[22] Z. Fang and K. Terakura, Phys. Rev. B **64**, 020509(R) (2001).
[23] T. Moriya, *Spin Fluctuations in Itinerant Electron Magnetism* (Springer-Verlag, Berlin, 1985), p. 54.
[24] A. J. Millis, Phys. Rev. B **48**, 7183 (1993).
[25] A. Ishigaki and T. Moriya, J. Phys. Soc. Jpn. **67**, 3924 (1998).
[26] To reduce the demagnetizing effect, we made the sample close to a cylindrical rod parallel to the c axis. In this case, the demagnetizing tensor is approximately $Nx = Ny = 1/2$, $Nz = 0$. The demagnetizing field Bd, is zero for the c-axis and approximately 0.6 $\mathrm{Wb/m^2}$ or 0.6 Tesla for the basal plane. This value is not large enough to be significant in our case.
[27] E. Stryjewski and N. Giordano, Adv. Phys. **26**, 487 (1977).
[28] For example, H. Yamada, Phys. Rev. B **47**, 11 211 (1993); K. Koyama *et al.*, *ibid.* **62**, 986 (2000).
[29] P. Coleman, Physica B **259–261**, 353 (1999); P. Coleman *et al.*, J. Phys.: Condens. Matter **13**, 723 (2001).
[30] T. Kimura *et al.*, Science **274**, 5293 (2001).

[31] The SdH signal is defined as $(\sigma-\sigma_b)/\sigma_b$ where σ is the conductivity and σ_b is the background conductivity. In addition, the usual fast Fourier analysis is inapplicable to the present case. The frequencies can, however, be determined by directly measuring the period of the oscillations, for example, for $B^{-1} \leqslant 0.05\ \mathrm{T}^1$.

[32] D. Shoenberg, *Magnetic Oscillations in Metals* (Cambridge University Press, Cambridge, 1984).

[33] For example, N. Harrison *et al.*, Phys. Rev. B **63**, 081101(R) (2001).